ELSEVIER

Biophysical Chemistry 50 (1994) 345–360

Biophysical Chemistry

The role of the potassium inward rectifier in defining cell membrane potentials in low potassium media, analyzed by computer simulation

J. Siegenbeek van Heukelom

Graduate School Neurosciences Amsterdam, Institute of Neurobiology, Group Cell Biophysics, University of Amsterdam, Kruislaan 320, 1098 SM Amsterdam, The Netherlands

(Received 26 April 1993; accepted in revised form 30 November 1993)

Abstract

A model is presented that describes the contributions of the potassium conductance and the Na^+/K^+ pump to the steady state magnitude of the plasma membrane potential, V_{rest}, at different concentrations of potassium in the extracellular fluid: K_o. The particular properties of the potassium inward rectifier, IKR, are shown to explain that V_{rest} frequently depolarises on lowering K_o below a critical value, because the IKR is only conductive when V_m is near to the potassium equilibrium potential or more negative. The model aims at a generic description of the process based on compartmental analysis. It is worked out to describe V_{rest} in mouse muscle fibres. Sensitivity analysis demonstrates that the process of switching off the IKR depends critically on the margin between V_{rest} and E_K, allowed for the IKR to remain open and the power of the Na/K pump to keep this margin small during the reduction of K_o. However, cells exposed to K_o just higher than the critical value may eventually also depolarize due to excessive loss of potassium. The model also demonstrates that loss of potassium membrane selectivity after blocking the Na/K pump by ouabain requires a mechanism additional to the above mentioned properties of the inward rectifier.

Key words: Computer simulation; Potassium; Inward Rectification; Na/K-pump; Membrane potential; Ouabain

1. Introduction

In many cells at rest the dominant potassium membrane permeability is due to the presence of open inward rectifying potassium channels (IKR) in the cell plasma membrane. These channels open when V_m is equal to or more negative than the potassium equilibrium potential and close at more positive values. Noble published the first successful computer-assisted, heuristic model description of the contribution of the IKR conductance to the membrane potential of cardiac cells, and its influence leading to the depolarisation of the membrane potential V_m in low potassium media [1,2]. Since then, a number of similar more accurate models have been produced to explain or describe the heart action potential and its propagation. Meanwhile, inward rectifying currents and channels have been found in many other cell systems. In a number of publications the direct current–voltage relationship has been measured [3–6]. Other publications report the

SSDI 0301-4622(93)E0104-D

observation of depolarisation on lowering the medium potassium concentration [7–11], the existence of two stable values of V_m in the same preparation [8,12], the observation of hyperpolarisation from a low to high V_m (negative inside) on stimulation of the cell [13], or the increase in Na/K pump site density on systemic reduction of K_o in the culturing medium [14]. Furthermore, there is a continuing discussion why some types of skeletal muscle fibres hyperpolarise and others do not [7–10] when K_o is reduced. If the properties of the IKR, indeed, form the main origin of the dichotomy in V_m as a function of K_o, one must conclude from these papers, that, leaving apart experimental differences, this potassium channel does not always exhibit exactly the same behaviour in all cells [15]. At the same time it is found so frequently in so many cell types, that it is most unlikely that this phenomenon depends critically on detailed molecular structures of the channels. So, the question arises: "Is inward rectification of this potassium channel alone sufficient to explain the observed dichotomy in V_m?"

As described by Jack et al. [16], any conductive cation system exhibits inward rectification as soon as its "controlling step" determining its resistance is located more at the intracellular side of the membrane than at the extracellular side. So, a broad range of molecular channel structures may exist to explain inward rectification. It has been described in a great variety of cells such as cardiac cells [1,4,8,12,17,18], starfish egg cells [19], skeletal muscle fibres [3,7,9,10,11,20–23], osteoclasts [5], neurones and glial cells [6,13,24], epithelial cells [25], erythrocytes [26] and macrophage cells [27]. This might also be why frequently this type of membrane conductance has been given different names such as "$I_{K,leak}$" in textbooks, "I_{K1}" in cardiac cells [16,18], "anomalous rectifier: AR" [10,20], inward rectifier K^+ channel, IRK [27], and more complex according to molecular description [15]. For reasons of generality, the name "inward K^+-rectifier IKR" (and the current through it I_{KR}) is preferred here.

Given the particularly strong dependence of the IKR on V_m and K_o it is impossible to describe the functional dependence of V_m on the extracellular ion concentrations in an explicit form. All variables are mutually dependent, prohibiting an identification of what are the dependent and independent variables in the, now classic, equations given by Goldman, Hodgkin and Katz ([28] Eq. (4.13)) and Mullins and Noda ([28] Eq. (4.16)). Not withstanding this difficulty, these equations still apply to a system in steady state. Moreover the Na/K pump that maintains the disequilibrium in the concentrations of sodium and potassium also depends kinetically on K_o [28].

Whereas recent detailed models to explain cardiac rhythmicity [29–32] include IKR, they are frequently so heavily connected with experimentally obtained results, that the generic question about the relationship between ion concentrations, membrane potentials and ion conductances is overshadowed by the details. Likewise, they do not deal with conditions where K_o is reduced. Consequently, investigators in other fields hesitate to exploit these models, when they observe in their cell systems similar peculiarities as mentioned above but do not dispose over such a wealth of experimental data.

The present contribution investigates what characteristic properties of IKR make V_m depolarise on lowering K_o. As a framework for formulating the influence of IKR on cellular homeostasis, the system is broken down into easy identifiable elements, which can simply be exchanged and mathematically reformulated. In its turn, the model may indicate what properties and elements will contribute to the depolarization of V_m. This study investigated only those properties of IKR as function of time, that do not exhibit short lasting transient behaviour.

Voltage clamp and patch clamp studies have revealed several properties of IKR and have led to a number of detailed descriptions concerning its molecular structure and functioning [3,15, 23,27,33–38]. The model uses a rather simple analytical relationship resembling the analysis by Hagiwara and Takahashi [19]. Furthermore, for sake of simplicity, the model treats the cells as non-polar and without unstirred layers adjacent to the membrane.

As most "macroscopical" cellular membrane conductances the total potassium conductance is

composed of several kinds of potassium conductances exhibiting each their own kinetics and sensitivities. These kinetics can be traced down to the open/close probabilities of the individual ion channels in the membrane that respond according to their own sensitivities to transmembrane potential (voltage sensitive channels) or other stimuli. The channels that underlie IKR are a clear example of such voltage sensitive channels. The moiety of the channel that is endowed with this ability is thought to possess a so-called "gating charge" [33,39,40], that moves in the electrical field created by the membrane potential. By statistical summation of all open and closed channel possibilities, using the Boltzmann distribution, one obtains the macroscopical conductance. Usually the characteristic elements for the macroscopical current are formulated by the membrane potential when the conductance is half-maximal (here: V_h (mV)) and the slope of change (here: V_s (mV)). The value of the gating-charge is inversely related to the slope [39]. Such approach has turned out to be very fruitful and can be applied to most channels known. However, the partition function may be much more complex if there are more choices than only "open" and "close". The model does not introduce this type of complexity, because experimental data do still not definitely make clear how this complex behaviour should be described. Moreover, the singularity in the dependence of V_m on K_o occurs so frequently, that precise details of channel kinetics can not be the origin of this singularity. Whereas at V_{rest} IKR dominates, the closure of IKR will produce a new steady state V_m and make other ion currents (including other types of potassium currents, like the calcium-activated potassium current I_{KCa}) to become more apparent. This introduction makes clear that the rather colloquial expression "IKR closes", used frequently, should be understood as "the "closed"-probability in the ensemble average of all inward rectifying potassium channels of the cell becomes larger". The expression "switch-off" means that "the closed probability becomes heavily predominant".

This contribution breaks down into five parts. Section 2 presents one new experimental graph, showing the basic phenomenon of the dichotomy in V_{rest} frequently observed experimentally by us and others [1,7–10]. Section 3 introduces the model in generic terms based on the principles of compartmental analysis. The elementary relationships of this generic model are open for redefinition, when such relationship has experimentally been determined and formulated. Section 4 demonstrates the implementation of the model for mouse skeletal muscle fibre with the relationships specifically applicable to that situation. Section 5 analyzes the sensitivity of the model for the choice of the individual parameters. In this section it is also demonstrated that the two versions of the model introduced in section 3.2, one for long-term flux measurements and one for short-term voltage-clamp measurements, are complementary. In section 6 the results are discussed and a number of possible refinements, that might be proposed on grounds of data dealing with elements of the total model. It also provides a prediction, that has turned out to be likely on grounds of data being published after the simulations were made.

2. Experimentally measured responses of V_{rest} to different K_o

To make the basic observation understandable, in Fig. 1 the values of V_{rest}, measured with intracellular microelectrodes in lumbrical muscle fibres of mice, are plotted at different K_o values on a semi-logarithmic scale. All experimental procedures are the same as described previously [10]. Down to 2 mM, V_{rest} decreases steadily with K_o following a slope of 55 mV/decade.

At K_o values between 1.0 and 2 mM, V_{rest} may be depolarized (to −52 mV) or hyperpolarized (about −94 mV), but below $K_o = 1.0$ mM only depolarized V_{rest} values were found. Similar relationships have been found in other cells [1,7–10,24] and this effect will be called here "switch-off". Such switch-off would not be observed if all membrane permeabilities remained constant [16,28,39,41]. Deterioration of cells is not the reason for this dichotomy (or singularity) of the dependence of V_{rest} upon K_o [10]. Sometimes V_{rest} starts to hyperpolarise on applying low K_o,

but depolarizes later without any apparent reason. After returning to the control solution, this behaviour can be re-evoked in the same cell. Additionally, blocking the Na/K pump with ouabain can also depolarize V_{rest} to a value of about −52 mV, along with a strong reduction of the relative potassium selectivity as has also been reported [10,11,42].

3. Methods and generic description of the model

3.1. Used program and computer

The simulation package used (STELLA™; version 2.10 (High Performance Systems, Lyme, New Hampshire 03768, USA) running on Apple Macintosh) is based upon a compartmental analysis approach to integrate step-wise differential equations. The routinely provided fourth-order Runge–Kutta method is used in the model. The graphic presentations of the simulation results in this paper were made with a more sophisticated program; in figures showing data as a function of time, the calculated points are concealed under the fitting curves. The simulation program does not contain more advanced integration algorithms to vary dynamically the scaling of the integration steps [30,31]. Because conductance and voltage changes differ in time by several orders of magnitude ([28] p. 13) from ion concentration changes, simulations that incorporate both might be either time consuming or to suffer from numerical instabilities. To overcome this problem, two complementary versions of the model were used. One version was for the voltage clamp simulations (assuming no change in cell concentrations due to simulation protocol). The other was for the ion-substitution experiments, taking advantage of the fact that in these experiments always electroneutral replacements of one salt by another in the medium were made.

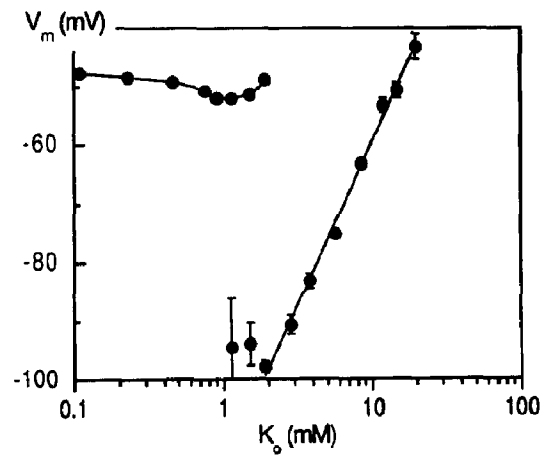

Fig. 1. Experimentally measured dependence of V_{rest} on K_o in the lumbrical muscle fibres of mice. The slope of the line fitting V_m values for $K_o \geq 2$ mM is 55 mV/decade. In the range between 1 and 2 mM K_o depolarization as well as hyperpolarization was obtained, whereas below 1 mM only depolarized V_{rest} was found. Bars represent ± standard error of the mean ($n = 6$).

3.2. Structure of the model

The general scheme used in the model is presented in Fig. 2.

The model is built with three types of equations: conservation equations, force-flux equations and one equation describing the steady state kinetics of the Na/K pump. The conservation equations are all derived from the general equation that integrates the influx of charge ($I = \Sigma I_j$, with the ion species $j = Na^+, K^+, Cl^-$) onto the membrane capacitance ($C = C_m S$ with C_m the specific membrane capacitance and S the surface of the cell) changing the membrane potential (V_m). Likewise it integrates the efflux of molecules (J_j, with charge z_j; F is the constant of Faraday) onto the volume of the cell (V) changing their concentration (c_j):

$$\begin{aligned} V_m(t) - V_m(0) &= -\int_0^t (I/C)\,dt' \\ &= -\int_0^t \left(\sum_j I_j/(C_m S)\right) dt' \\ &= -\int_0^t \left(\sum_j F z_j J_j\right)/(C_m S)\,dt' \\ &= -\int_0^t \left(\sum_j z_j\, dc_j(t')/dt'\right)(FV/C_m S)\,dt' \end{aligned} \quad (1)$$

The general form of all force-flux equations for passive diffusion is still formulated with use of the constant-field flux equation [16,28,41]:

$$J_j = U\left(c_{ji}\, e^U - c_{jo}\right) P_j/(e^U - 1), \quad (2)$$

where $U = z_j FV_m/RT = z_j V_m/0.025$, P_j is the membrane permeability for j; subscript o and i stand for outside and inside the cell, respectively.

The formulation of P_j incorporates all voltage or concentration dependencies of permeabilities (especially those of IKR). The model does not assume active transport or particular voltage-dependent conductance changes for chloride and applies Eq. (2) directly to this ion with a constant value for P_{Cl}. For sodium and potassium, active transport by the Na/K pump adds, with the proper sign, $3J_{pump}$ to J_{Na} and $2J_{pump}$ to J_K. Concentration dependence on Na_i and K_o of J_{pump} is implemented with the equation frequently used in simulations [31,32],

$$J_{pump} = J_{p,max}(1 + K_{mK}/K_o)^{-2} \times (1 + K_{mNa}/Na_i)^{-3}, \quad (3)$$

thus introducing three parameters for the model: the maximal pump-activity: $J_{p,max}$ and the affinity constants for Na_i: K_{mNa} and for K_o: K_{mK}. As a first approximation, the dependence of J_{pump} on V_m [28,43] is not installed and P_{Na} is a constant.

The relation between changes in V_m and c_j due to membrane fluxes of ion j is

$$\left(\frac{dV_m}{dt}\right)_j = \frac{\phi_d FV}{C_m S}\frac{dc_j}{dt} = q\frac{dc_j}{dt}. \quad (4)$$

Included in q is a factor ϕ_d that allows for an adaptation for inaccessible space in the cell. It was taken as being 1 in the voltage clamp version and as 0.9 in the ion flux version rather arbitrary until a better determination is available. Normally q (dimension V/M) in this equation, relating the electrical changes to the concentration changes of individual ionic fluxes, is so large, that

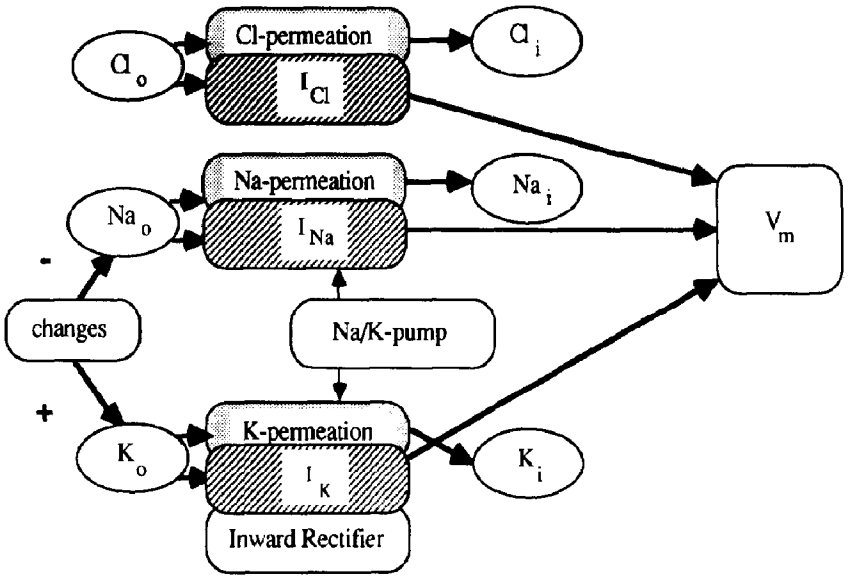

Fig. 2. Schematic presentation of the model, showing the changes, fluxes and integrations in the model. "Changes" represents the exchanging of K^+ by Na^+ or vice versa. To mimic the fact that experimentally such changes take some time, the step function is smoothed with a time constant of about 8 s (except in Fig. 5b, where this constant is varied). Cl_o, Na_o, K_o, Cl_i, Na_i and K_i represent the concentrations of chloride, sodium or potassium outside or inside the cell. Cl, Na and K permeation represent the fluxes of these ions (Eq. (2); fluxes represented here as arrows); the concomitant electrical currents are I_{Cl}, I_{Na} and I_K (and related arrows). Whereas intracellular concentrations are obtained by integration of the fluxes, the changes in membrane potential (V_m) are effected by integration of the electrical current (Eqs. (1) and (4)). The contributions of the Na/K pump to I_{Na} and I_K are derived from Eq. (3). The contribution of IKR to potassium permeation is explicitly shown and is implemented by Eq. (7). In the voltage clamp version the changes were kept zero, but a command signal $V_{command}$ (not shown in this figure) is imposed upon V_m by a current: $I_{command} = gain(V_{command} - V_m)$ injected in the V_m compartment to keep $V_m = V_{command} \pm 1\%$. In this version the real conversion between fluxes and currents (q from Eq. (4)) is used and the total actual time could be reduced to seconds.

small changes in concentration are associated with a large change in V_m. This poses stringent limitations to the stability of the numerical integration: time steps for integration in electrical terms should be essentially much shorter than the time steps one would like to use in the simulation of flux experiments. As all parameters are electrically heavily fed back by Eqs. (1) and (2) (see also section 1), one can assume that the fast electrical processes are always in steady state on the time scale of the slower diffusional processes [28]. Therefore, a reduction of the value for q in the flux simulations will not considerably change the outcome. This was verified (see section 5.1) and led to the installation of two separate versions of the model: one mainly for the description of ion substitution experiments (taking $q \approx 1\%$ of the proper value) and the other for the simulation of voltage clamp experiments (with q as the proper value).

The model uses values for the relative membrane permeabilities for K^+, Na^+ and Cl^- obtained from the literature. Trial-runs of the model provided parameter values to fit to other data available from the literature, such as the intracellular concentrations (see Fig. 3). By this method one needs to specify only one absolute permeability value, which can be deduced from the measurement of the permeability or of the conductance of the membrane for one ion that is described by the model (see section 4.1.).

An expression for the potassium permeability: P_K, is needed, that contains the relation of the IKR to its most important parameters: its conductance when fully opened, the steady state open/close partition function of the channels, and a residual permeability (P_o) when IKR is fully closed.

Conductances can be described as chord conductance [16,41] defined as $g_{K(chord)} = I_K/(V_m - E_K)$ or as slope conductance $g_{K(slope)} = (\partial I_K/\partial V_m)$. For V_m near E_K (i.e. V_m-$E_K \approx 0$) the difference vanishes (E_K being the equilibrium potential for K^+), $g_{K(chord)} \approx g_{K(slope)}$. P_K is related to g_K by the following approximation [16,41]:

$$P_K = g_K RT/(zF)^2 c_{K,membrane}. \quad (5)$$

The K^+ concentration in the membrane, $c_{K,membrane}$, can be approximated by the logarithmic average between the concentration on either side: in the cell ($c_{K,i}$) and outside ($c_{K,o}$) [41]:

$$c_{K,membrane} = (c_{K,o} - c_{K,i})/\ln(c_{K,o}/c_{K,i}). \quad (6)$$

The dependence of P_K on K_o and V_m is defined similar to the expression proposed by Hagiwara and Takahashi [19] for g_K,

$$P_K = P_o + \left(\bar{P}_K/\sqrt{K_o}\right)\left[1 + \exp(V_m - V_h)/V_s\right]^{-1}. \quad (7)$$

P_o is the residual potassium permeability needed in the model to account for the experimentally observed fact that closure of the IKR let V_m depolarize to about -50 mV instead of to the equilibrium potential of Na^+, $E_{Na} \approx +60$ mV (see Fig. 1). The appropriate value was $P_o \approx 4P_{Na}$. As mentioned in section 1, this residual permeability may consist of a number of conductances, which may be open already or become opened because of the depolarization of V_m (like I_{KCa}).

The function in the denominator of the right-hand side of Eq. (7), $(1 + \exp(V_m - V_h)/V_s]$, is the steady state open/close partition function of the channels according to the Boltzmann distribution. In principle one can incorporate in this function all steady state kinetic peculiarities of the IKR, such as its gating mechanism [3,15,17,23,33,34,36], its dependence on K_o [3,4,7–11,19,22] and its ion-selectivity [18,35,37]. In Eq. (7) V_h is the value where this term is half-maximal. The parameter V_s, frequently called the slope parameter, defines the sensitivity of the partition function for the energy differences (here $V_m - V_h$) and is related to the gating charge [33,39]. Hagiwara and Takahashi [19] showed that over a wide range of K_o values V_h differed by a constant value from E_K: so, V_h depends on K_o. In section 4 the values V_h and V_s will be adapted to values in skeletal muscle fibres. In the sensitivity analysis (section 5) the influence of the choice of V_h and V_s will be considered. More complex kinetics will be discussed in section 6.

The value K_o enters the expression of P_K explicitly because of the factor $\sqrt{K_o}$ and implicitly because it also affects V_h, that is dependent on E_K. The first term of the description of the

permeability of IKR, $\bar{P}_K/\sqrt{K_o}$, represents the maximal permeability of IKR when $(V_m - V_h)/V_s \ll 0$ (and the partition function ≈ 1). It has been observed frequently that $\bar{g}_K$ (the maximal conductance of IKR) varies proportionally to the square root of K_o [4,18,19,36,39]. In view of Eqs. (5) and (6), the most appropriate way to include this fact is to install $\sqrt{K_o}$ in the denominator of this component. $\bar{P}_K$ allows the scaling of the total model in such a way that at one value of K_o this component fits with the experimentally observed value.

The process of voltage clamping was simulated by including a voltage command mode, injecting electrical current into the cell to keep $V_m = V_{command}$ within 1%. The experimental uncertainty in this situation as to which ions carry the injected current, and the short duration of the current injection, made us assume that the current injection does not affect the intracellular concentrations.

The model simulates delays, normally induced by diffusion or by mixing processes in many experimental studies, by smoothing the step-function that simulates the changes of the medium composition (see Fig. 2 and section 4.3).

In the model no explicit boundary conditions were introduced ensuring constant osmotic pressure in the cell and only inspection of the total change of intracellular K^+, Na^+ and Cl^- ions was carried out. The most important reasons for not imposing stringent osmotic limitations are: (1) most experimental data do not provide information about this aspect; (2) it is likely that cells swell or shrink when the concentrations vary; and (3) volume- and osmo-regulation by means of ion-cotransporters are very likely to occur in reality [44], but functional relationships to be inserted in the model are missing as yet.

4. The model applied to skeletal muscle fibres

4.1. Installation of the model

In this section the model is applied to a simulation of the resting potential V_{rest} in mouse skeletal muscle fibres using data from the literature and our own observations. The complex definition of V_h introduced here is applicable to this section but is no prerequisite to demonstrate that lowering K_o leads to a depolarization (see 5.2.2). The fibre was described as a cylinder in Eq. (4); using the following values: $r = 17.5$ μm [45] and $C_m = 8$ μF/cm² [46]. The relation between the electrical and concentration changes is $q = \phi_d FV/C_m S (= Fr/2C_m) = 10552$ V/M, with $\phi_d = 1$. From ref. [21] the ratios $\alpha_m = P_{Na}/P_K = 0.01$ and $P_{Cl}/P_K = 3$ were taken to apply to the control situation (here $K_o = 5.7$ mM). The value of g_K at 100 mM K_o, as provided by Standen and Stanfield [3] (3.4 mS cm^{-2}), was used to scale P_K according to the experimental value of 7.6×10^{-6} cm/s using Eqs. (5) and (6) and taking $K_i = 175$ mM (see Fig. 4a). Their g_K values in media with different potassium concentrations were fitted with an equation comparable to Eq. (7) and provided the dependence of V_h on K_o. For $K_o > 10$ mM the values for V_h differed by a constant value from E_K, comparable with data obtained by others [19,31,32]: $V_h - E_K = \Delta V_{h,K=high} = -24$ mV. For K_o is 2.5 and 10 mM $V_h = -72$ mV [3], and with $K_o = 2.5$ mM $V_h > E_K$. Voltage clamp data in the literature do not provide much information about V_h at values of K_o lower then 2.5 mM, because of the difficulty to measure the reduced currents through IKR when K_o is low. The assumption that V_h remains constant for all $K_o \leqslant 10$ mM would imply that the partition function of Eq. (7) becomes a constant provided that V_m also levels off. This would imply that P_K becomes approximately a constant and V_m behaves as described by the classic Goldman–Hodgkin–Katz equation [28,41]. A hyperpolarized V_{rest} means that P_K remains sufficiently large or, alternatively formulated, $V_m - V_h/V_s$ sufficiently small (Eq. (7) and section 5.2.2). The model assumes that from about 10 mM downwards V_h begins to differ again from E_K, but now positively (with as maximal constant value $\Delta V_{h,K} = \text{low} = +30$ mV). This rather complex relationship between V_h and E_K was described again with a Boltzmann-like function for the dependence of V_h on K_o (see curve "V_h" in Fig. 4c):

$$V_h = E_K + \Delta V_{h,K=low} - \frac{2(\Delta V_{h,K=low} - \Delta V_{h,K=high})}{1+\exp(K_{co}/K_o)}. \quad (8)$$

The value K_{co} represents the cross-over concentration of K_o, where $V_h \approx E_K$ (see Fig. 4: $K_{co} \approx 13$ mM).

As slope parameter in Eq. (7) was chosen $V_s = 9$ mV, which is equivalent to a "gating charge" of 2.8 [28,33,39].

The Na/K pump was characterized by taking $K_{mK} = 1$ mM [47] and adjusting $J_{p,max}$ and K_{mNa} to obtain an integrated set of values for c_j and V_{rest}, comparable to experimentally determined values, at $K_o = 5.7$ mM [10,48]: 130 mM $< K_i <$ 150 mM; 7 mM $< Na_i <$ 20 mM; 5 mM $< Cl_i <$ 7 mM; $-77 < V_{rest} < -74$ mV (the value of V_{rest} determines directly Cl_i by means of the Nernst equation). The values $J_{p,max} = 50$ pmol/cm^2 s and $K_{mNa} = 7$ mM were chosen (see Fig. 3) and used routinely further for all simulations. Fig. 3d demonstrates two important aspects: J_{pump} is, under all conditions specified, never more than 30% of $J_{p,max}$ and under control conditions the choice of $K_{m,Na}$ is not very important anymore.

4.2. Dependencies on K_o

The changes induced by substituting K_o for Na_o, or vice versa, in the steady state values of

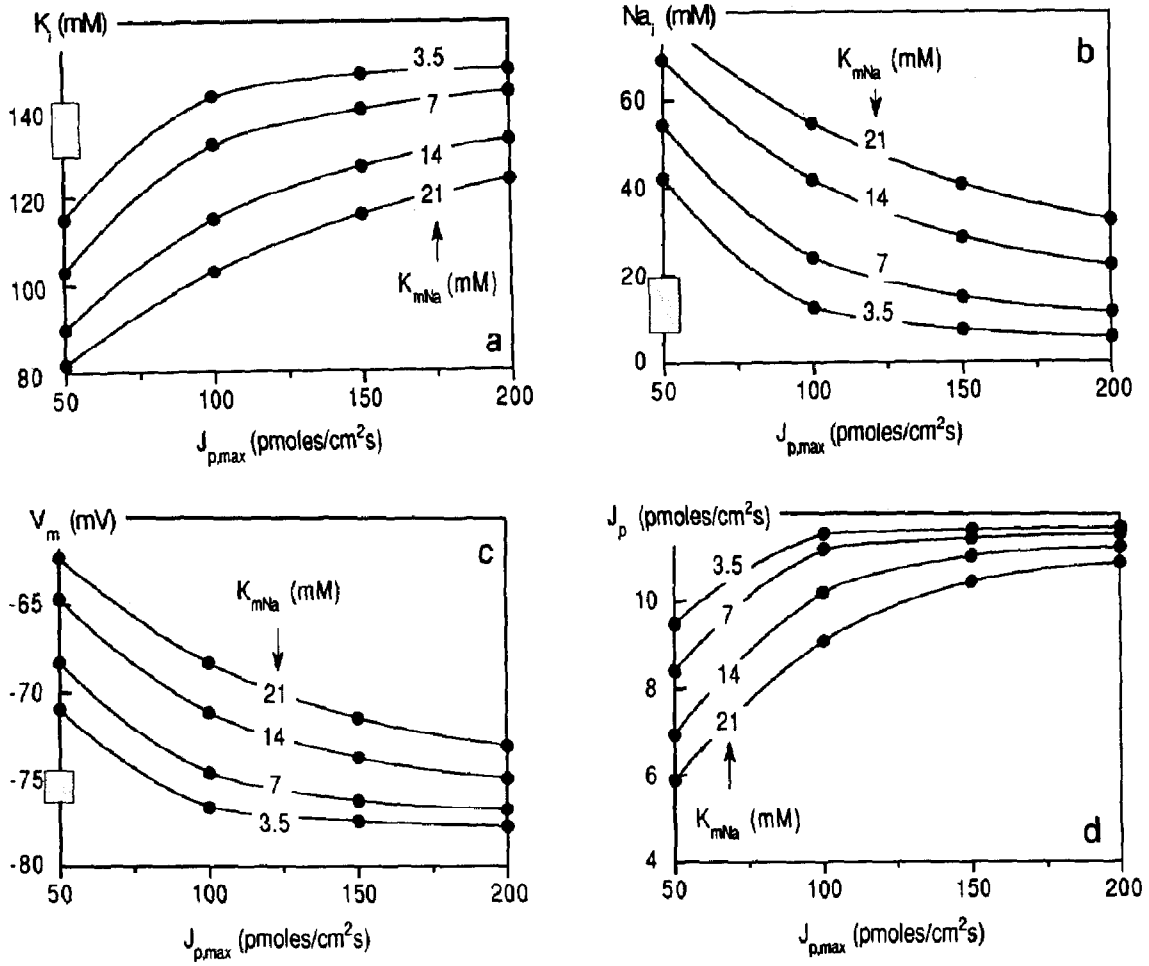

Fig. 3. Dependence on $J_{p,max}$ (ranging 50 to 200 pmol Na/cm^2 s) and K_{mNa} (3.5, 7, 14 and 21 mM) of: (a) K_i (mM); (b) Na_i (mM); (c) V_m (mV); (d) J_p (pmol/cm^2 s). The experimental values for K_i, Na_i and V_m are indicated by a bar on the vertical axis in each panel; the choice $J_{p,max} = 150$ pmol Na/cm^2 s and $K_{mNa} = 7$ mM makes the simulated values fall in the indicated range. All values presented were obtained at the end of 1800 s simulations. Values for Cl_i are not shown: they can be found using the Nernst equation and fall in the range as specified.

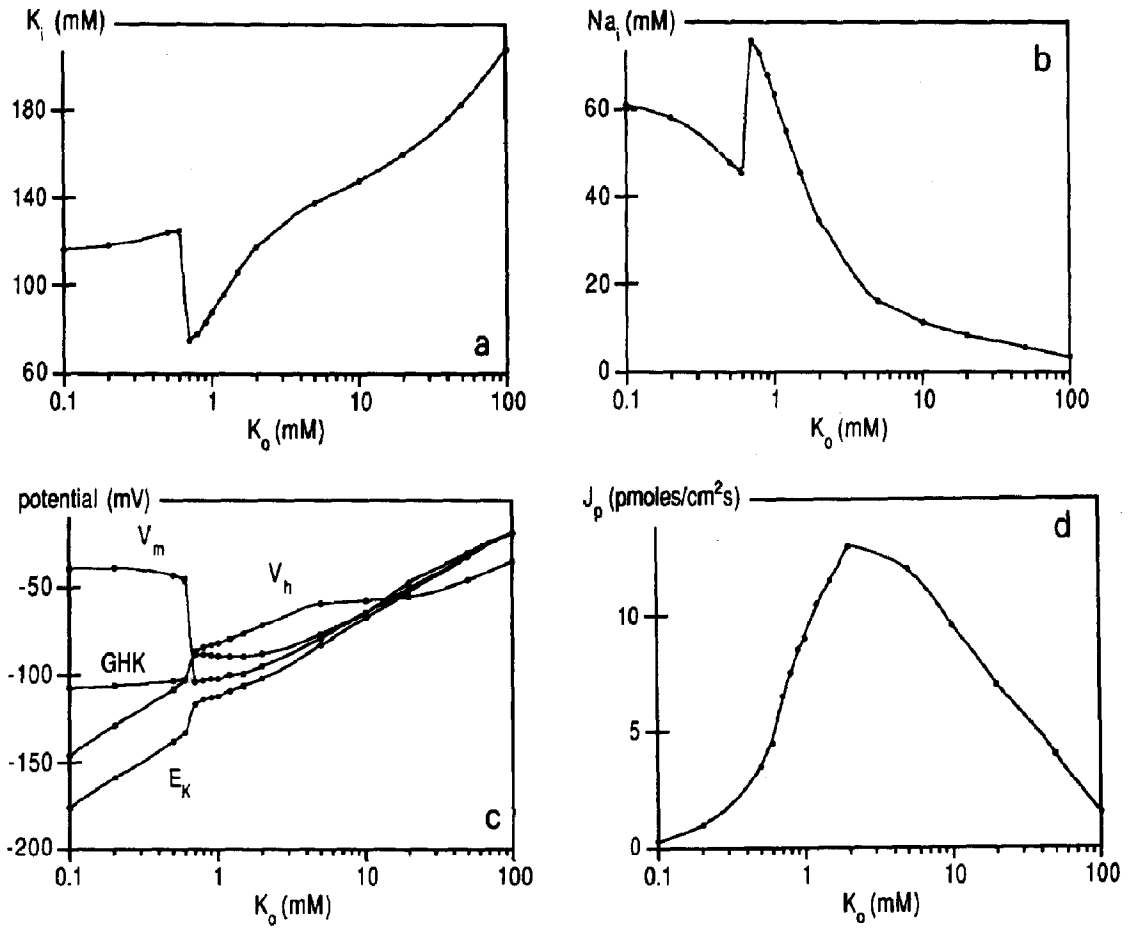

Fig. 4. Dependence of cellular parameters, calculated 2900 s actual time after the change in K_o from 5.7 mM, on the K_o value specified on the horizontal axis: (a) K_i; (b) Na_i; (c) V_m, V_h, E_K, GHK and (d) J_p. Curves were obtained by smoothed interpolation; for J_p two lines were used: one from 0.1 to 2 mM K_o and one for $K_o > 2$ mM. The curves in panels a, b and c show deviations near the switch-off value, $K_o = 1$ mM, because a fully steady state in this critical range is not attained after 50 min; to attain such values unrealistic long times are required. When K_o decreases, K_i decreases as well, until IKR closes. Then K_i increases again. The response of Na_i mirrors that of K_i. Increased Na_i can compensate for the reduced stimulation of the Na/K pump by K_o. Cl_i closely follows V_m (see panel c). In panel c GHK represents the membrane potential calculated from K_i and Na_i using the GHK equation with a constant P_K/P_{Na} ratio (= 100). The curve V_h closely follows Eq. (8); at $K_o \approx 13$ mV $V_h = E_K$.

K_i, Na_i and J_{pump} are displayed in Fig. 4 as functions of K_o. Several aspects can be identified. J_{pump} has its maximal value in the range between 5 and 2 mM and starts to decline at about 2 mM K_o as can be seen in Fig. 4d, but also in Figs. 4a and b where at this concentration K_i and Na_i begin to deviate from the extrapolation of curves obtained at higher K_o values.

When K_o is lowered below the critical value of 0.7 mM the closure of IKR leads to an increase of K_i, though the electrochemical gradient increases due to both its electrical and chemical component. The consequence of the reduction in J_{pump} is also visible in the curves for V_m, and GHK in Fig. 4c and particularly in E_K demonstrating a hump in this part of the curve. GHK is calculated using the Goldman–Hodgkin–Katz voltage equation [39,41] with $\alpha_m = P_{Na}/P_K = 0.01$ and the new steady state values of K_i, Na_i and Cl_i; all as a function of K_o. In Fig. 4c the value of V_h is also shown. The sum of the intracellular monovalent ion concentrations remains compara-

ble to the initial value when K_o is between 0.6 and 10 mM.

Because V_h decreases with decreasing K_o, according to Eq. (8) a switch is always observed. The exact value of K_o, where this switch occurs, can be influenced by the properties of IKR (for instance, its dependence on V_s and V_h) and those of the Na/K pump (for instance, its dependence on K_{mK} and $J_{p,max}$). Instead of scaling further the unknown parameters to fit as good as possible our own experimental results, in section 5 the influence of the critical parameters on the behaviour of the simulated cell is analyzed. In addition, experimental data [18,49,50] suggest that insertion of a dependence of IKR on intracellular ion concentrations might be more appropriate (see section 6).

4.3. Influence of chloride on V_m responses to cation substitutions

In the model, chloride distributes passively and it should not influence the value V_{rest}. However, the chloride permeability does influence the velocity with which V_m can respond to ion changes in the medium. This is illustrated in Fig. 5a, where increasing P_{Cl} leads to a slowing down of the speed of depolarization induced by a sudden increase of K_o. The results compare qualitatively well with observations made by Hodgkin and Horowicz ([21] Fig. 9). Thus, the process of redistribution of intracellular chloride slows down the readjustment of V_m to a value near E_K. If K_o changes fast compared to the response time of V_m, the difference between V_m and V_h, that follows E_K (Eq. (8)), immediately exceeds the critical value in Eq. (7) and P_K drops to P_o leading to a direct cell depolarisation ("Fast" in Fig. 5b). When K_o changes more gradually (two curves called "Slow" in Fig. 5b), it may take a considerable time (> 2 h) to find out that the hyperpolarized V_m is not a stable value. Then V_{rest} depolarizes due to loss of intracellular potassium because IKR remains open (the total P_K being larger than in the control situation as it depends on $1/\sqrt{K_o}$: cf. Eq. 7). Experiments [10] where K_o was first reduced to 1.9 mM, and after 30 min to 0.76 mM, did not show such accommodation.

4.4. Voltage clamp experiments

Because the description of the properties of IKR is based on a number of published voltage-clamp experiments, it was worthwhile to see to

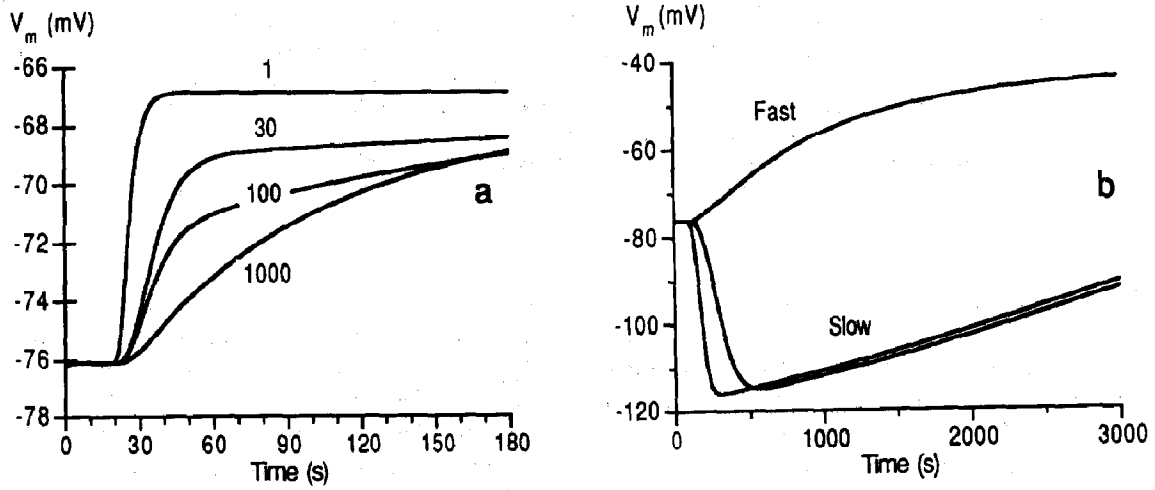

Fig. 5. The influence of Cl^-. (a) P_{Cl} (values in the curves are P_{Cl}/P_{Na}) delays the depolarization of V_m in response to increasing K_o (at $t = 20$) from 5.7 to 8.55 mM. (b) When P_{Cl} is large (300 P_{Na}), lowering K_o quickly to 0.7 mM can lead to a depolarization of V_m ("Fast": smoothing the step function, that simulates the change in ion composition, with a time constant of 4 s) whereas lowering K_o slowly leads to an hyperpolarization ("Slow": two curves with smoothing time constants of 40 and 140 s, respectively). "Smoothing" is a routinely provided function in the program.

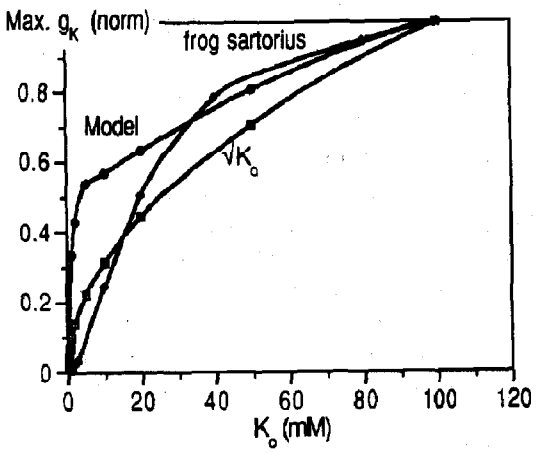

Fig. 6. Voltage clamp results. The dependence of $\bar{g}_K$ of K_o is compared with $\sqrt{K_o}$ and the experimental data for sartorius muscle [3]. All values are normalized to 1 for $K_o = 100$ mM.

what extent the voltage clamp version of the model can simulate the findings of these studies. The model simulated the experiments of Standen and Stanfield [3] at $Cl_o = 0$ by taking $P_{Cl} = P_{Na}$. In the voltage clamp version the values obtained for I_{KR} were divided by $V_m - E_K$ to produce g_K and not calculated from P_K according to Eq. (7). The data are presented in Fig. 6a together with the function $1/\sqrt{K_o}$ and the data from ref. [3]. All curves are normalised to make their values 1 for $K_o = 100$ mM; the value of $\bar{g}K$ found with $K_o = 100$ mM is about two times larger then the actual value from [3]. The dependence of the simulated $\bar{g}_K$ on K_o compares better with the square root curve than with the data of the experiments. Once IKR is fully opened at hyperpolarised V_m, the normal Goldman–Hodgkin–Katz equation can describe $\bar{g}_K$ as function of V_m [16,28,39,41]. In Fig. 6 the voltage clamp responses were calculated with intracellular concentrations equal to the values, when $K_o = 5.7$ mM. Calculations with the actual steady state values as given in Fig. 4 showed only 10 to 15% deviations from the values in Fig. 6.

4.5. The effect of ouabain

Experimentally, ouabain induces a greater depolarization in skeletal muscle fibres [10,42] than the 1 mV predicted by the usual straightforward theoretical analysis [28]. The instantaneous effect of ouabain was simulated by turning $J_{p,max}$ to zero and Fig. 7a shows that the model calculation gives an initial depolarization of about 1 mV. In

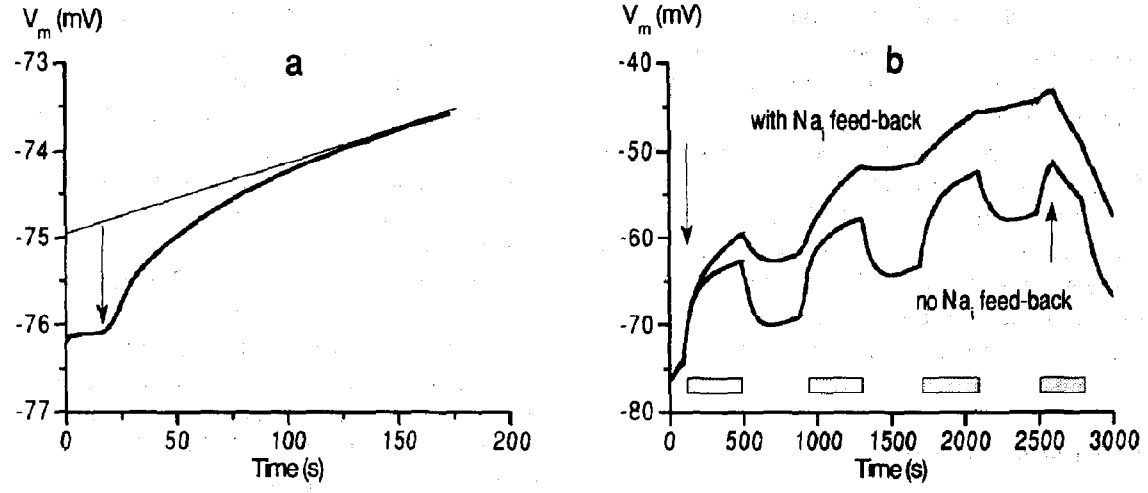

Fig. 7. The influence of ouabain. (a) When the Na/K pump is stopped ($J_{p,max} = 0$ pmol/cm^2 s at $t = 20$) the initial depolarization, specified as the difference (arrow) between V_{rest} ($t \leq 20$) and the value at $t = 20$ of the line, tangent to the curve at 180 s, amounts about 1 mV. (b) The "long-term" response of V_m to ouabain (applied between $t = 100$ and 2600: see arrows). Periodical changes in K_o from 5.7 to 8.55 mM (bars) induce variations in V_m that give an impression of the selectivity ratio P_K/P_{Na}: this ratio being correlated to the size of the response. Two conditions were compared: (1) "no Na_i feed back": when P_K is described as in this paper (Eq. (7)) and the ratio does not show a decrease, and (2) "with Na_i feed back": when P_K is multiplied by a factor ($Na_{i,control}/Na_{i,exp}$) thus simulating the condition that P_K is inhibited by Na_i.

Fig. 7b the simulation of V_m during longer exposures to ouabain is shown. The response of V_m on varying K_o between 5.7 and 8.55 mM (150%) gives an impression of the selectivity ratio $\alpha_m = P_{Na}/P_K$. Experimentally, these responses of V_m to such variations in K_o decreased continuously after ouabain application (0.1 mM) indicating that this ratio increased [10]. In the simulation curve indicated by "no Na_i-feedback" the responses remained constant, indicating that according to the model P_{Na}/P_K is not increased by inhibition of the pump alone. Here the depolarization is due to a drop in E_K, and by the definitions of V_h (Eq. (8)) and P_K (Eq. (7)) there is no reason for a closure of IKR because V_h and V_m follow E_K closely, thus keeping the partition function small. The second trace in Fig. 7b shows that the decrease in K^+-selectivity can be mimicked, in this case by installing a reduction of P_K by increasing Na_i [18,50]. It compares rather well with the experimental observation ([10], Fig. 7). Another alternative, increase of P_{Na} by increasing Na_i, as suggested by others [42] is also possible and can be simulated as well. Kawata and Hatae [51] demonstrated that addition of Ba^{2+} to the medium perfusing frog skeletal muscle leads to an initial increase of the membrane resistance (likely due to the closing of IKR by Ba^{2+}) followed by a sodium-dependent decrease due to a tetrodotoxin-resistant Na-conductance, suggesting that both effects may occur.

The situation decribed here differs strongly from the depolarisation of V_m, when a action potential is generated [16,18,30–33,39]. Then V_m depolarizes due to an enormous increase in sodium conductance of the membrane. In terms of the model, IKR is dragged into the region where it closes according to its definition.

5. Sensitivity analysis

5.1. Comparison of the flux version and voltage clamp version

The statement that one may reduce the ratio q, relating the concentration changes to the electrical changes, in the ion flux version of the model to 1% was verified by comparing the responses of the simulated intracellular concentrations and V_m on substitutions to K_o values of 0.1, 1, 10 and 100 mM with $q = 1\%$, 10% or 100% of the proper value. In all cases the differences were smaller than 0.3%; this was also the influence of different values of q during fast changes in the flux model (see Fig. 5). Most likely, the decrease of q does not lead to very different results because ion substitution experiments do not violate electroneutrality and all electrical sources and drains reside in the same cell membrane.

5.2. Variations in the definition of the kinetic elements of the model

The sensitivity of the model was investigated to variations in a number of critical parameters such as the affinity constants for Na_i and K_o of the Na/K pump, the parameters in Eq. (8) describing the opening and closing of IKR and the dependence of the open channel conductance on K_o (Eq. (7)).

5.2.1. The sensitivity for the kinetic constants of the Na / K pump

According to Fig. 3, with the choice of $J_{p,max} =$ 150 pmol Na/cm^2 s and $K_{m,Na} = 7$ mM and $K_{m,K} = 1$ mM, the dependent variables are rather insensitive of the choice of $J_{p,max}$ and $K_{m,Na}$ for a cell at rest in control medium.

Once V_m was steadily depolarized at $K_o = 0.5$ mM doubling $J_{p,max}$ did not switch V_m from a depolarization to a hyperpolarization, suggesting that under these circumstances stimulation of the pump is not very critical.

Whereas the sensitivity of the Na/K pump was taken throughout this paper as $K_{mK} = 1$ mM, simulations compiled in Fig. 8 demonstrate that lowering this parameter also changes the switch-off to lower K_o. K_{mK} determines at what concentration the pump power declines (see Fig. 4d, where apparently this decline already starts at $K_o = 2$ mM). Therefore it appears that this affinity and the sensitivity of V_h to K_o determine the switch-off value. With appropriate choices of V_h and K_{mK}, IKR can switch off before the pump activity declines considerably on lowering K_o and, paradoxically, K_i increases on reducing K_o.

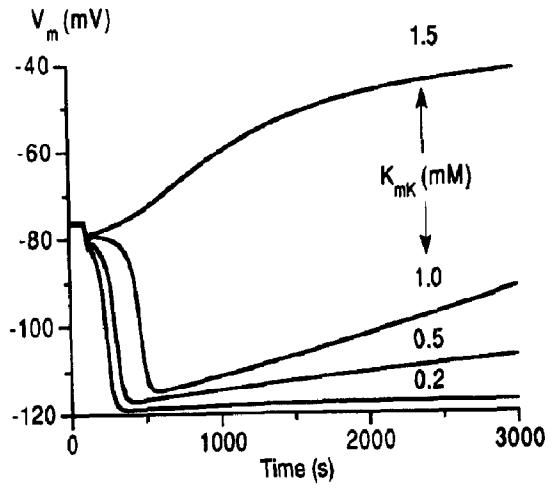

Fig. 8. The influence of the choice of K_{mK}. Responses of V_m to a reduction of K_o to 0.7 mM at $t = 100$ with different K_{mK} values: 0.2, 0.5, 1.0 and 1.5 mM. The curve with $K_{mK} = 0.2$ mM shows almost no decline, whereas the curves with $K_{mK} = 0.5$ and 1.0 mM decline slowly and with $K_{mK} = 1.5$ mM depolarization starts immediately.

5.2.2. *The sensitivity for the steady state kinetics of IKR*

V_h, adapted in the simulation to fit data from the literature for skeletal muscle fibres (Eq. (8)), is only one particular solution of the model. To estimate the influence of V_h in more general terms, the model was run with several different, and simpler, definitions for V_h. The conclusion is that the switch-off occurred, as long as the quotient $(V_m - V_h)/V_s$ became sufficiently positive. Any definition where V_h follows E_K in some way or another will lead to a value for K_o where this will occur. This was checked by using of Eq. (8) the relationships $V_h = E_K + 30$ mV (the maximal value of Eq. (8)) and $V_h = E_K - 24$ mV (the minimal value of Eq. (8)): in both cases the switch-off occurred when decreasing K_o.

The value of V_s determines the difference between V_m and V_h needed for the switch-off and the related K_o value. This value was found to decrease when V_s increases (studied were 4 mV, 6 mV, 9 mV (standard) and 13 mV, representing gating charges of about 6, 4, 3 and 2 elementary units, respectively).

Redefining V_h according to the formalism of Goldman, Hodgkin and Katz [16,28,39,41] as $V_h = (RT/F)\ \ln[(K_o + \alpha_h Na_o)/(K_i + \alpha_h Na_i)]$ allowed a more detailed examination of the dependency of the critical K_o value on V_h. The entity α_h represents the selectivity of V_h for Na^+ with respect to K^+. Now V_h levels off at low K_o, as described normally for V_m with constant P_{Na} and P_K. The selectivity ratio α_h in this definition may be compared with the one used to calculate V_m ($\alpha_m = (P_{Na}/P_K)_m = 0.01$, at $K_o = 5.7$ mM, is used in the model: section 4.2). When $\alpha_h = 0$, $V_h = E_K$ and V_m depolarized on reduction of K_o. With the settings of the model $\alpha_h < 0.012$ let V_m depolarize whereas $\alpha_h > 0.013$ let it hyperpolarize, even with $K_o = 0.1$ mM. This last situation is no true steady state, because the Na/K pump could not cope with the loss of potassium through IKR.

5.3. *Sensitivity of the conductance of the open IKR channel*

It is clear from Fig. 6 that the similarity of the simulated g_K values and the experimental data from frog sartorius muscle is not very strong, partly because these data are not proportional to the square root of K_o. Simulations without the value $1/\sqrt{K_o}$ in the definition of the open IKR permeability (Eq. (7)) made g_K a nearly linear function of K_o. The omission introduced quantitative differences in K_i, Na_i and V_m as function of K_o, but it did not abolish the switch-off at sufficiently low K_o.

5.4. *The influence of the experimental procedure*

The model suggests that the experimental method of changing the medium composition can influence considerably the outcome of the experiment and that the time needed to obtain a true steady state might be excessively long. Though Fig. 8 covers a simulation time of 50 min, runs for twice that time showed that in the cases of $K_{m,K} = 0.5$ mM and 1 mM, V_m eventually depolarized when $K_0 = 0.7$ mM with opened IKR due to loss of intracellular potassium and was still depolarizing at the end of the simulation. Even the data of

Fig. 4 for K_o values very near to the switch-off are still not from a true steady state. This and discrepancies in the speed of change in K_o might explain that hyperpolarized as well as depolarized V_m values have been reported in the range of K_o around the switch-off value [1,7–10,24].

6. Discussion

6.1. Inward rectification of IKR is sufficient to explain the switch-off

Section 4.5 suggests that the Na/K pump itself is not directly needed to explain the switch-off, but the disequilibrium in ion concentrations effected by it. The observed dissociation between the switch-off and loss of intracellular potassium (section 5.2.1) corroborates this conclusion. Additionally, the analysis with different formulations of the partition function (5.2.2) suggests that it occurred provided that this function becomes large enough. As long as V_h depends primarily on E_K, such situation is always found by decreasing K_o sufficiently. In all aspects IKR functions as a positive feed-back element in the cellular ion-homeostasis. When activated it stabilizes V_m. If V_h levels off at low K_o values, and both, V_h and V_m, can be described by a properly formulated logarithmic function (see section 5.2.2) the partition function becomes a constant. Whether this will lead to a switch-off or not depends strongly on the value of V_s. This might be why in a number of cells [7,21,52] the switch-off is not observed. It might interesting to compare the molecular structures of the IKR of such cells with those from depolarising cells.

Sections 5.3 and 5.4 suggest that even when V_h "follows" E_K, there is a range of K_o values where IKR remains open with excessive loss of intracellular potassium, with which the Na/K pump cannot cope. Kennedy et al. [14] reported that the $(Na^+ + K^+)$-ATPase density in the cell membrane can vary depending on K_o with a maximum in this particular range. This suggests that a continuous heavy loading of the Na/K pump may produce a regulatory signal for the incorporating more pump sites in the membrane.

6.2. Introducing more complex elementary relationships

The model presented can simulate most recordings reported earlier [10] concerning the behaviour of V_m as function of K_o. It is more important, that it also opens ways of investigating differences in IKR that might explain the differences generally found in such measurements [7,21,52]. For simplicity only, several relationships described in the literature have been omitted: active chloride transport [53], osmoregulation depending on the (frequently electroneutral) handling of the ions featuring in the model [44]. Also the behaviours of the two main elements in the model have been reduced to nearly caricature. One is the Na/K pump, exhibiting explicit dependence on V_m [43] and a very complex kinetic behaviour usually described by the "Post-Albers scheme" and analyzed in full detail by the late Peter Läuger [28]. The other is IKR self, demonstrating fast and transient kinetic behaviour [18,36], multi-site kinetics [33,39] (including cooperativity) and gating by intracellular magnesium [55]. All these properties were not included partly because such relationships are not yet cast in analytical forms, let it be over the total range of K_o values presented here and for the same preparation. The results of the three previous sections nevertheless suggest that without introducing all these complexities the phenomenon of "switch-off" becomes understandable. Section 4 illustrated how the amount of computational details tends to overgrow the conceptual background of the model, though nothing, except speed of computation, will hinder their introduction.

As for muscle cells, an additional complexity may exist: the model treats the fibres as non-polar, whereas there is experimental evidence that the major portion of the conductive IKR is located in the T-system (for recent discussion, see ref. [23]). Therefore the extrusion K^+ in the T-tubuli might be enhanced. Given the constricted structure of the tubuli the potassium concentration there might be slightly higher then in the medium: K_o. This would make the switch-off of the I_{KR} even more pronounced.

6.3. Predictive value of the model

In the section on ouabain it has been demonstrated that without an additional relationship in the model, the experimentally observed reduction in potassium selectivity cannot be understood. Changes in intracellular concentrations may provide the signal for this reduction as has been shown by including an inhibition of I_{KR} by Na_i. This possibility that Na_i and/or K_i modify the behaviour of IKR might also explain the spontaneous depolarization of V_m following an initial hyperpolarization in low K_o, due to Na_i increase and K_i decrease during this initial hyperpolarization. Inhibition of IKR by Na_i (see 4.5) has now been found experimentally [50].

In conclusion, the model can simulate the switch for hyperpolarization to depolarization, observed in a number of cell types, when K_o is lowered. It shows that this phenomenon mainly depends on the sensitivity of the open/close partition function of the inward rectifying potassium channel to the electrochemical potassium gradient across the cell membrane. This sensitivity can be described by a Boltzmann distribution function with the parameters V_h (the membrane potential when the partition function is half maximal) and V_s ("the slope" quantifying the speed of change in the function [28]). V_h can be described with simple as well as complex equations (like Eq. (8) in this paper) without losing the aspects of the general observation.

Acknowledgement

The author is grateful to Dr. W.J. Wadman, Dr. B.L. Roberts, and Dr. H.V. Westerhoff for critically reading of and commenting on the manuscript, and Dr. P.C. Diegenbach for computational advise and the use of the Macintosh IIfx.

References

[1] S. Weidmann, Elektrophysiologie der Herzmuskelfaser (Huber, Bern, 1956).
[2] D. Noble, J. Cell. Comp. Physiol. 66 (1963) 127.
[3] N.B. Standen and P.R. Stanfield, Pflügers Archiv 378 (1978) 173.
[4] M. Mazzanti and L.J. DeFelice, Biophys. J. 54 (1988) 1139.
[5] S.M. Sims and S.J. Dixon, Am. J. Physiol. 256 (1989) C1277.
[6] N. Uchimura, E. Cherubini and R.A. North, J. Neurophysiol. 62 (1989) 1280.
[7] T. Akiyama and H. Grundfest, J. Physiol. London 217 (1971) 33.
[8] D.C. Gadsby and P.F. Cranefield, J. Gen. Physiol. 70 (1977) 725.
[9] P.P. Nánási and M. Dankó, Pflügers Archiv 414 (1989) 157.
[10] J. Siegenbeek van Heukelom, J. Physiol. London 434 (1991) 549.
[11] H. Mølgaard, M. Stürup-Johansen and J.A. Flatman, Pflügers Archiv 383 (1980) 181.
[12] J.R. McCullough, W.T. Chua, H.H. Rasmussen, R.E. Ten Eick and D.H. Singer, Circ. Res. 66 (1990) 191.
[13] J.M. Sullivan and E.M. Lasater, J. Neurophysiol. 64 (1990) 1758.
[14] D.G. Kennedy, J.K. Aronson, J.G. Bloomfield and D.G. Grahame-Smith, Biochim. Biophys. Acta. 1027 (1990) 218.
[15] C. Miller, Science 252 (1991) 1092.
[16] J.J.B. Jack, D. Noble and R.W. Tsien, Electric current flow in excitable cells (Clarendon Press, Oxford, 1975).
[17] J.R. Balser, D.M. Roden and P.B. Bennett, Biophys. J. 59 (1991) 150.
[18] E. Carmeliet, G. Biermans, G. Callewaert and J. Vereecke, Experientia 43 (1987) 1175.
[19] Hagiwara and K. Takahashi, J. Membr. Biol. 18 (1974) 61.
[20] B. Katz, Arch. Sci. Physiol. 3 (1949) 285.
[21] A.L. Hodgkin and P. Horowicz, J. Physiol. London 148 (1959) 127.
[22] S. Hestrin, J. Physiol. London 317 (1981) 497.
[23] H. Matsuda and P.R. Stanfield, J. Physiol. London 414 (1989) 111.
[24] T. Brismar and V.P. Collins, J. Physiol. London 460 (1993) 365.
[25] F. Lang, G. Messner and W. Rehwald, Am. J. Physiol. 250 (1986) F953.
[26] P. Christophersen, J. Membr. Biol. 119 (1991) 75.
[27] Y. Kubo, T.J. Baldwin, Y.N. Jan and L.Y. Jan, Nature 362 (1993) 127.
[28] P. Läuger, Electrogenic ion pumps (Sinauer, Sunderland, 1991).
[29] D. DiFrancesco and D. Noble, Philos. Trans. Roy. Soc. London B 307 (1985) 353.
[30] M.R. Guevara and H.J. Jongsma, Am. J. Physiol. 258 (1990) H734.
[31] R.L. Rasmusson, J.W. Clark, W.R. Giles, E.F. Shibata and D.L. Campbell, Am. J. Physiol. 259 (1990) H352.
[32] R.L. Rasmusson, J.W. Clark, W.R. Giles, K. Robinson,

R.B. Clark, E.F. Shibata and D.L. Campbell, Am. J. Physiol. 259 (1990) H370.
[33] B. Hille and W. Schwarz, J. Gen. Physiol. 72 (1978) 409.
[34] S. Ciani, S. Krasne, S. Miyazaki and S. Hagiwara, J. Membr. Biol. 44 (1978) 103.
[35] G. Eisenman and R. Horn, J. Membr. Biol. 76 (1983) 197.
[36] B. Sakmann and G. Trube, J. Physiol. London 347 (1984) 641.
[37] M.J. Kell and L.J. DeFelice, J. Membr. Biol. 102 (1988) 1.
[38] P. Gates, K. Cooper, J. Rae and R. Eisenberg, Progr. Biophys. Mol. Biol. 53 (1989) 153.
[39] B. Hille, Ionic channels of excitable membranes, 2nd Ed. (Sinauer, Sunderland, 1992).
[40] P. Läuger, in: Single-channel recording, eds. B. Sakmann and E. Neher (Plenum Press, New York, 1983) p. 177.
[41] S.G. Schultz, Basic principles of membrane transport (Cambridge Univ. Press, Cambridge, 1980).
[42] S.R. Seabrooke, M.R. Ward and N.K. White, Quart. J. Exp. Physiol. 73 (1988) 561.
[43] D.C. Gadsby, J. Kimura and A. Noma, Nature 315 (1985) 63.
[44] E.K. Hoffmann and L.O. Simonsen, Physiol. Rev. 69 (1989) 315.
[45] C. Juel, Muscle Nerve 11 (1988) 714.
[46] A. Dulhunty, G. Carter and C. Hinrichsen, J. Muscle Res. Cell Mot. 5 (1984) 315.
[47] O.M. Sejersted, in: The Na^+,K^+ pump, Part B. Cellular aspects, eds. J.C. Skou, J.C Nørby, A.B. Maunsbach and M. Esmann (Liss, New York, 1988) p. 195.
[48] P.J. Donaldson and J.P. Leader, Pflügers Archiv 400 (1984) 166.
[49] I.S. Cohen, D. DiFrancesco, N.K. Mulrine and P. Pennefarther, Biophys. J. 55 (1989) 197.
[50] H. Matsuda, J. Physiol. London 460, (1993), 311.
[51] H. Kawata and J. Hatae, Japan J. Physiol. 40 (1990) 853.
[52] K. Kuba and M. Nohmi, Br. J. Pharmacol. 91 (1987) 671.
[53] G.L. Harris and W.J. Betz, J. Gen. Physiol. 90 (1987) 127.
[54] H. Matsuda, Ann. Rev. Physiol. 53 (1991) 289.